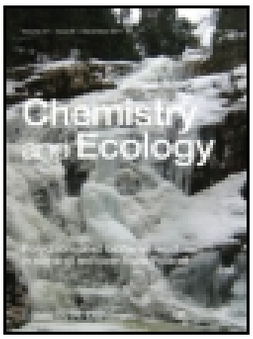

Chemistry and Ecology

ISSN: (Print) (Online) Journal homepage: https://www.tandfonline.com/loi/gche20

Exploration of haematite-loaded rice husk biochar as a low-cost nanosorbent to remove Cr (III) from the aqueous media

Tunzeel Iqbal, Fozia Batool & Shahid Iqbal

To cite this article: Tunzeel Iqbal, Fozia Batool & Shahid Iqbal (2023): Exploration of haematite-loaded rice husk biochar as a low-cost nanosorbent to remove Cr (III) from the aqueous media, Chemistry and Ecology, DOI: 10.1080/02757540.2023.2188205

To link to this article: https://doi.org/10.1080/02757540.2023.2188205

Published online: 27 Mar 2023.

CHEMISTRY AND ECOLOGY
https://doi.org/10.1080/02757540.2023.2188205

Taylor & Francis
Taylor & Francis Group

RESEARCH ARTICLE

Exploration of haematite-loaded rice husk biochar as a low-cost nanosorbent to remove Cr (III) from the aqueous media

Tunzeel Iqbal [a], Fozia Batool [b] and Shahid Iqbal [c]

[a]Department of Chemistry, The Rawalpindi Women University, Rawalpindi, Pakistan; [b]Institute of Chemistry, University of Sargodha, Sargodha Pakistan; [c]Department of Chemistry, University of Education Jauharabad Campus, Jauharabad, Pakistan

ABSTRACT

In this study, the biochar of rice husk was modified to a nanosorbent upon loading with haematite for Cr (III) removal from aqueous solutions. Three adsorbents, rice husk, rice husk biochar and haematite-loaded rice husk biochar, were used for equilibrium adsorption studies. SEM and FTIR analysis revealed the presence of pores and various surface active sites on a nanomaterial, which were responsible for the adsorption of Cr (III). C–H, –O–H, C=O stretching vibrations were observed in characterised FTIR peaks. Modelling of adsorption isotherms indicated best fit for Freundlich isotherm with maximum Kf value of 12,218 and 39.5 for linear and non-linear nanomaterial experimental calculations, and positive n value in range of 1–10 for all forms of adsorbents, Dubinin–Radushkevich adsorption saturation capacity q_s showed high readings of 9417 and 76.8 for haematite nanomaterial, Elovich isotherm favoured non-linear results in case of nanomaterial with increased Q_m values 43.4–112.3 from raw form to nanosorbents and Temkin isotherm with. Kinetic and Thermodynamic results were also summarised. Constants k and h and Q_e capacity were tabulated for Pseudo second order model with highest Q_e in the range of 20.36–22.52 for haematite loaded biochar nanomaterial. Hence, haematite based rice husk biochar nanostructure was employed as an efficient adsorbent for uptake of chromium.

ARTICLE HISTORY
Received 9 September 2022
Final Version Received 3 March 2023

KEYWORDS
Haematite loaded nanomaterials; rice husk; biochar; chromium; adsorption; kinetics and thermodynamics

Introduction

In the earliest days of scientific research various methods like coagulation, distillation, precipitation, were employed to prepare or synthesise nanomaterials, such as charcoal or alumina based, but those methods were time taking, costly and limited [1].

Now a day, an important topic is the applications of nanostructures in the global energy demand. In recent years, nanotechnology and nanomaterials have wide range of exploration in the industrial sector. This is attributed to significant benefits over old repeated methods such as geometrical complexity and customisation. Owing to large surface area, size of particles iron based nanoparticles such as those of haematite and magnetite as magnetic material have become demand of the present research era [2].

CONTACT Tunzeel Iqbal tunzeel.iqbal@f.rwu.edu.pk The Rawalpindi Women University, Rawalpindi 43600, Pakistan

Furthermore, chitosan based iron, silica and various functional groups modified nanomaterials have also been employed in recent research fields, indicating high demand in nanomaterials modifications [1]. Common applications of nanoscience are in automobile, aerospace, defense components, medical, household and energy sector [3].

Production of biochar from plant biomass has gained importance owing to its dryness, porosity and large surface area. Its physical characteristics depend upon chemical composition of feedstock. Loss of chemically bound moisture and thermal decomposition of organic feedstock occurs above 120°C, while breakdown of cellulose occurs over 240–350°C, for lignin over 280–500°C and hemicellulose over 200–260°C [4]. The composition and structure of biochar depends upon nature of feedstock and operating parameters such as pretreatment, that is, drying and chemical activation, rate of heating, pressure, highest temperature of treatment (HTT), reaction containing vessel conditions such as dimensions, catalysts, orientation and stirring, reaction residence time, flow rates of gases and post treatment methods such as crushing, mesh size and biochar activation. All these factors are important but pyrolysis at HTT contributes more significantly to determine final adsorption surface of biochar, because the discharge of volatile material, formation and evaporation of the intermediate products are all dependent on temperature. However, temperature changes and its range for all steps vary with the form of biosorbents material [5].

Chromium is stable in the environment mostly in trivalent and hexavalent forms. Chromium and its compounds have been widely used in many industries like textiles, leather tanning, metallurgy, photography, electroplating and in pigments. According to EPA concentration of chromium in drinking water is almost 0.05 mg per Litre. Chromium enters into the human body through ingestion, inhalation and dermal absorption. Exposure occurs mainly through inhalation and dermal contact. Whereas, in general population exposure occurs through ingestion of chromium contents from soil, water and food. Chromium absorption is dependent on its oxidation state and nature of its compounds. Industrial effluents contain toxic metals in free or compound forms. These toxic metals are used in textile and tannery industries and due to poor industrial waste treatment technology, these are discharged into water bodies such as surrounding river banks.

Effluents comprise of carcinogenic metals, which can become part of food chain and exhibit their toxic effects unless removed from source of pollution [6]. Effluents discharged from industries can also alter physical and chemical properties of natural water streams such as pH and oxygen contents. Tanneries and textile industrial effluents mostly consist of lead, cadmium, iron, chromium, zinc and nickel which act as human carcinogens and also accumulate in agricultural soil to affect quality production of crops [7].

Conventional methods used for removal of metals have some drawbacks, which include use of chemicals in large quantities for precipitation, slow rate of precipitation of metal, poor condition of settling and accumulation of metal precipitants. For all methods, a common difficulty is the continuing environmental problem of sludge disposal in large quantity. Which creates another problem of aqueous solution to solid waste pollution with no recovery of separated metals [8]. Adsorption is significant when immobilisation or fast elimination of impurities is required at reasonable or little amounts [9]. Agricultural and animal wastes have been used as adsorbents and recently, researcher's attention is to produce a low cost adsorbent called biochar with several environment

friendly applications in adsorption processes [10]. In adsorption, substances are bound through physical or chemical interactions to solid surface. Hence, it is a mass transfer process and an efficient method for the treatment of effluents [11]. Several low-cost adsorbents have been derived from industrial processes, agricultural waste, natural products, or different biopolymers and activated carbon and applied to remove toxic metal ions from polluted or contaminated water [12]. Recently, heavy metals have been removed by agricultural feedstock by biosorption process. Sorption process describes a set of processes, which comprises of sorption and precipitation methods involving the transmission of ions from liquid phase to the solid surface phase.

The efficiency of biomass to remove metals is due to presence of lignocellulosic structures [13]. Hydroxyl and amino groups, present in the structure of biopolymers, increase metal removal efficiency. Newly explored biopolymer adsorbents may be polysaccharide based-materials which are derived from chitosan, chitin and starch. Also polymers which have crosslinked structured hydrogels, are used for waste water purification [14]. Agricultural waste materials and industrial wastes are now focused for the remediation of heavy toxic metals due to ease in their accessibility and presence of chelated functional groups [15]. Use of ash or biochar of agricultural wastes is another addition to efficient biosorbents that can remove toxic metals from wastewater. Rice husk is composed of 74% organic and 26% inorganic components [16]. Organic portion includes cellulose, hemicelluloses, lignin, D-galactose, proteins, L-arabinose, methylglucuronic acid and vitamins. Inorganic constituents include 80% silica, 3.93% alumina, 3.84% calcium oxide, 1.45% potassium oxide, 0.78% sulphur trioxide, 0.67% sodium oxide and 0.25% magnesium oxide [17].

Formation of nanomaterials and their implementation fr metal removal have been reported in literature . Earlier nanomaterials silica an cobalt based have been employed for adsorption studies using rice husk and other biomass materials [18]. Present adsorption stud on nanomaterials and their use is based on further nanosised study and its successful use on chromium adsorpion.

The aim of present study is focused on remediation of Cr (III) by using three forms (RH, RHBC and HLRHBC) of rice husk adsorbent and equilibrium adsorption analysis for their applications on industrial scale. In this study haematite nanomaterial is loaded on rice husk biochar and its functionality as a novel nanomaterial is highlighted in calculated results for its use and implementation at scientific level.

Materials and methods

Pure analytical grade chemicals and reagents were utilised. Doubled distilled water was used for all experiments. Stock solution of Cr (III) was prepared by adding required amount of its salt named as chromium oxalate [Cr ($C_2H_4O_2$)] in 1000 mL flask. Standards in the range of 15–90 ppm were prepared by taking required amount of chemical reagent from stock solution and then diluted with distilled water. Then working solutions in required concentrations were prepared upon further dilution of standards. Adsorbent rice husk was collected from Punjab, Pakistan, washed away with distilled water to eradicate contaminants, dried in electric oven at 90°C for 24 h and ground to desired sieve size upto 60 mesh for adsorption experiments. Biochar of rice husk (RHBC) was prepared in electric furnace at 450°C which was then modified to haematite based nanomaterial

labelled as (HLRHBC) through a chemical process. For this purpose RHBC was suspended in 500 mL distilled water mixed with solution of iron chloride ($FeCl_3$) prepared by mixing 1.35 g of iron chloride with 500 mL deionised water and mixed thoroughly with pH (11) adjustment by using 0.1 M solution of sodium hydroxide (NaOH). After 60 min of continuous shaking mixture was filtered followed by washing with purified water and also ethanol. It stayed on drying in electric oven at 100°C for 24 h [19].

Characterisation of biosorbents

Rice husk (RH), rice husk biochar (RHBC) and haematite loaded rice husk biochar (HLRHBC) were categorised by Scanning electron microscope (SEM) and Fourier transform infrared (FTIR). Scanning electron microscopy determines macro porous structure and physical morphology of powdered solid. Surface structure and distribution of elements of sorbents in raw, biochar and nanostructure forms were determined by SEM. The surface active functional groups onto the surface of adsorbents were analysed using FTIR (Model Shimadzu AIM-8800) in 400–4000 cm^{-1} range by mixing solid with KBr to form pellets. Identification of functional groups is important because they are responsible for metal binding and uptake from solution. Brunauer–Emmett–Teller (BET) was performed for surface area and porosity of the adsorbent surface.

Adsorption study

Cr (III) sorption was observed for its solutions in the range of 15–90 ppm (100 mL) with three forms of rice husk sorbent (RH, RHBC and HLRHBC). Adsorption isotherms are used to give results of best fit of data, and are described as two factor isotherms such as Langmuir isotherm, Freundlich isotherm, Temkin isotherm, & Dubinin–Radushkevich isotherm and Halsey or three parameter isotherms such as Sips, Toth and also Redlich-Peterson. Linear and non-linear models are calculated to explain sorption process depending upon the curves whether, follow linearity or non-linearity terms according to experimental results. For linear and non-linear methods computer operations are used to perform isothermal parameters on Microsoft excel and spread sheets [20]. To describe experimental parameters in isotherms linear regression analysis is used. It shows a relationship among amount of sorbate and its concentration at equilibrium. Errors that results from linear regression analysis of linear forms of isothermal data can be eliminated by non-linear regression analysis, as an efficient tool. Non-linear analysis is now used in many applications such as effluents treatment, waste water etc. [21]. Different parameters are studied in non-linear isotherms by using correct formula of isotherm, which can eliminate biased results of linear analysis [22]. Kinetic parameters were studied for uptake of chromium by adsorbents for 10–70 min shaking of adsorbents containing chromium solutions. After experiments solutions were filtered and the filtrate was analysed by an Atomic Absorption Spectrophotometer. Experimental data were then used for the kinetic model. After adsorption experiments, the adsorbent contains contaminants that have to be removed or recovered from the adsorbent surface. Adsorbent can be reused after desorption, as the material used for desorption does not harm the adsorbent, but in some cases after use in the process, the sorption ability (removal efficiency) of adsorbent is reduced.

Results and discussion

Raw rice husk was converted to biochar by pyrolysis and biochar nanomaterial was prepared by loading ohaematite on it. All three adsorbents, that is, RH, RHBC and HLRHBC, were used to study the uptake of chromium through batch adsorption experiments. SEM characterisation was performed for the determination of functional active sites on the adsorbent surface, their position on the adsorbent and their surface fundamental distinctive properties such as porosity, structure and irregularity as an essential step (Figure 1).

Fourier transforms infrared (FTIR) spectra of untreated and treated rice husk were obtained before and after the adsorption of metal ions (Figure 2). In IR raw RH and RHB bands appear in the range of 2500–3000, indicating C–H stretching vibration for the aldehyde/alkane functional group. While those in the range of 3200–3700 are –O–H stretching vibrations which are weak and broad owing to the alcoholic group which is involved in intramolecular hydrogen bonding. IR for the removal of Cr (III) by RHB indicates peaks in these regions are reduced due to the uptake of metals on adsorbent sites and the involvement of these active functional sites in adsorption (Figure 3). Strong Peaks at 1715–1740 are due to C=O stretching vibrations of aldehyde/keto/carboxylic functional groups in the rice husk structure. Medium vibrations in the range of 1330–1440 correspond to O–H bending vibrations of carboxylic acids or alcohols. Medium peaks from 1020 to 1250 are due to the presence of C–N stretching vibrations of amines. At 3700 cm^{-1} or above free –OH groups exist. In FTIR spectra of HLRHB, a strong peak at 2926.01 cm^{-1} shows N–H vibrations as a result of stretching occurring in the range of 2800–3000 cm^{-1}. The C–N stretching peak also appears in FTIR spectra of HLRHB after the adsorption of Cr metal. A sharp peak in the region of 1705–1725 cm^{-1} is recognised to be either carboxylic or ketone C=O stretching vibrations. Also the peaks 3200–3700 cm^{-1} show O–H stretching vibrations of alcoholic or acidic groups [23]. IR results of spectra for HLRHB after the removal of metal were also observed and compared with FTIR of raw HLRHB. The number of peaks is reduced after adsorption due to the involvement of surface functional groups (Figure 4) as clear in the 3200–3700 cm^{-1} range of all spectra. Stretching and bending vibrations are observed in the range of 3400–1630 [24].

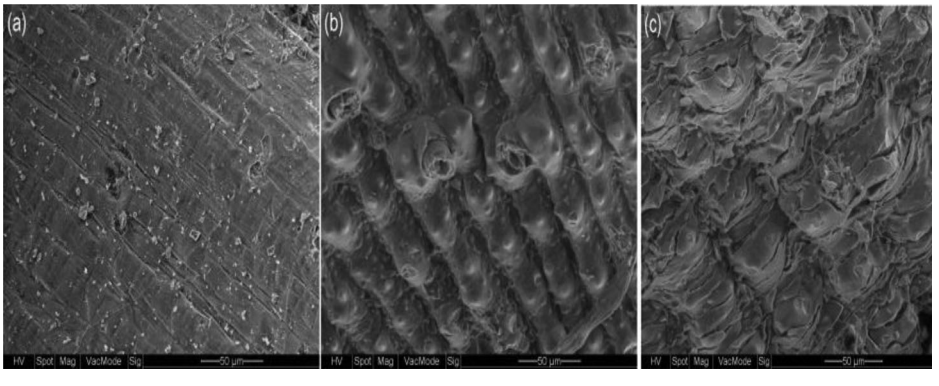

Figure 1. A. SEM image of raw form of rice husk (RH) B. image of Haematite loaded on rice husk biochar (HLRHBC) C. SEM image of rice husk biochar (RHBC).

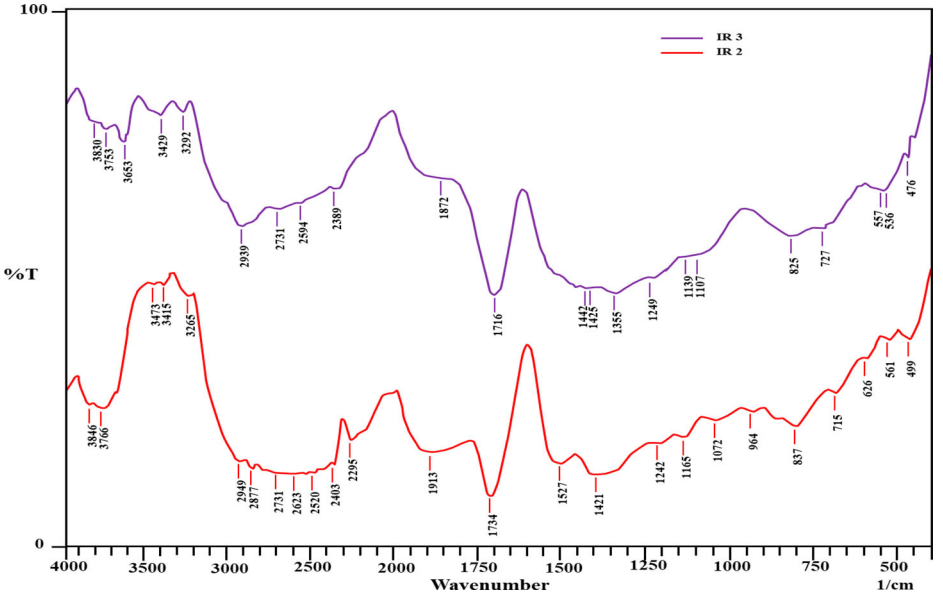

Figure 2. Fourier Transform Infrared spectrum of raw form of rice husk (RH) (IR 2 = before adsorption, IR 2 = after adsorption).

Peaks at 1300–1440 cm^{-1} are attributed to O–H bending vibrations of alcoholic or carboxylic groups. Medium peaks at 1020–1250 cm^{-1} are due to C–N stretching frequencies. Medium peaks of Fe–O are observed at 500–600 cm^{-1} and peaks 1800–2100 cm^{-1} show

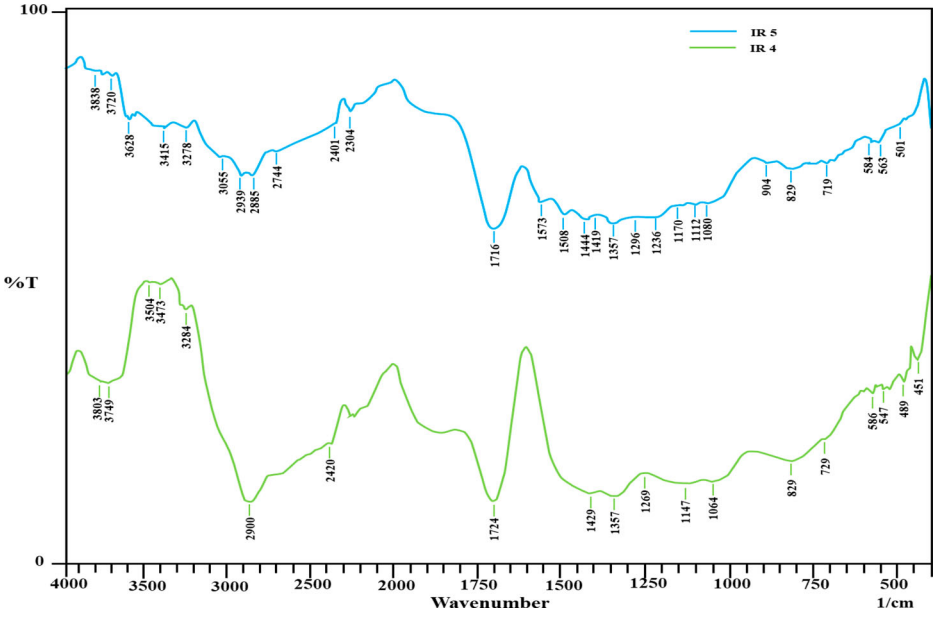

Figure 3. Fourier transform infrared spectrum of RHBC (IR 4 = before adsorption, IR 5 = after adsorption).

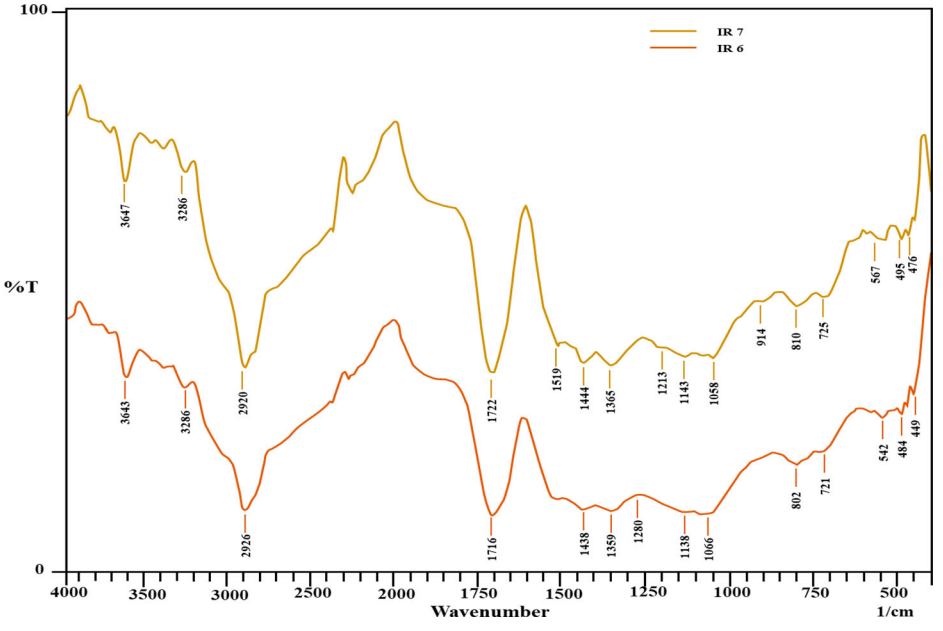

Figure 4. Fourier transform infrared spectrum of HLRHB (IR 6 = before adsorption, IR 7 = after adsorption).

metal carbonyl interaction. Because for the removal of metal ions oxygen-containing functional groups are needed, so metal adsorption is increased by using metal oxide nanoparticles on biochar [25].

BET analysis was obtained to get information about surface area. The results reveal the mesoporous surface for adsorbents with surface area increases due to treatment. The rice husk (RH) surface area was 2482 m^2/g, while RHBC was 2681 m^2/g and HLRHB was 2750 m^2/g. BET analysis also supports adsorption results.

Adsorption experiments

Adsorption study was accomplished by the batch-wise process for the remediation of chromium by different adsorbents form including haematite-based nanomaterials. In Figure 5. The removal of Cr (III) is depicted through the adsorption process. The removal was studied for an adsorbent dose of 1 g, at concentrations 15–90 ppm by keeping contact time and agitation speed constant at 60 min and 150 rpm, respectively. The removal efficiency was increased with an increase in solution concentration, showing the presence of a large surface area and more pore size on the sorbent surface which facilitates more metal adsorption. From Figure 5 it is predicted that rice husk has a good potential for Cr (III) removal from aqueous media. But RHBC showed less % removal than raw RH. It may be due towater vapours in raw sorbents that enhance their adsorption ability. But in RHBC due to pyrolysis volatile compounds are evaporated and pores are activated which promote metal adsorption. When compared with HLRHBC nanomaterial, the percent adsorption is high owing to the presence of surface functional groups that are actively involved in metal removal. The

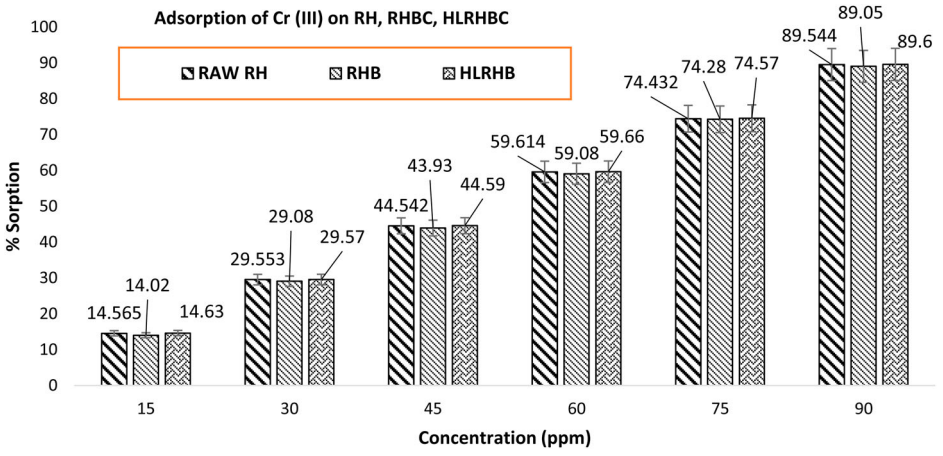

Figure 5. Comparison among three forms (raw RH, RH biochar and Haematite loaded RHBC) of rice husk biosorbents for the adsorption of chromium (III) upon variation in concentration (ppm).

enhanced adsorption capacity was observed owing to an increase in metal concentration due to the mass transfer effect [26].

Modelling of adsorption isotherms

Various isotherm models are available for analysing adsorption experimental data at equilibrium. Adsorption equilibrium conditions provide information about the sorption process. Also, sorption experimental data showing the adsorption of metals on adsorbents in relation to their concentration in solution could be explained by calculating the results of various adsorption isotherms.

Freundlich isotherm

To describe Freundlich isotherm experimental data were plotted against Log Cad and Log Ce to determine the values of constants K_F and n (Figure 6). The value of correlation coefficient R^2 indicates the extent of the adsorption process, also the high value of K_F shows more adsorption capacity of the adsorbent and $1/n$ indicates the strength of the adsorption process. When $1/n$ is between 0 and 1, it indicates favourable adsorption and a high value of K_F expresses the significant role of sorption functional groups on the sorbent surface. Also values of n in a series of 1–10 support the adsorption process and negative values indicate unfavourable adsorption by the linear form of Freundlich isotherm and experimental data should apply to the non-linear form of isotherm [27]. Values of Freundlich isotherm constants K_F and constant n were calculated from slope and intercept. High constant values indicate more rate of adsorption. Freundlich plots for chromium adsorption are shown below. These plots favours this isotherm owing to good R^2 values and favourable values of constants. $R^2 = 0.9696$ for HLRHBC shows the best removal of chromium through multilayer adsorption. Also the high value of K_F for HLRHBC suggests maximum adsorption of chromium on this nanomaterial with a value of $n = 0.9$, that is, close to 1, indicating the best fit to the model. Values of non-linear forms of Freundlich

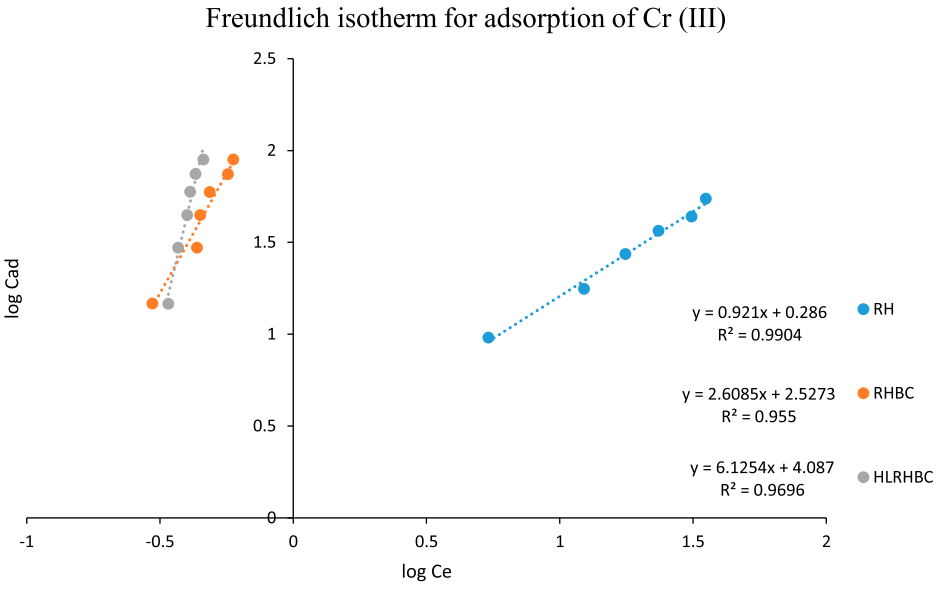

Figure 6. The Freundlich isotherm for the uptake of chromium (III) by RH, RHBC and HLRHBC.

constants are also given in Table 1 which also follows experimental results.

$$\text{LogCad} = \text{Log}K_F + 1/n \log Ce \quad \text{Linear Form} \tag{1}$$

$$C_{\text{ad}} = \text{KFCe}^{1/n} \qquad \text{Non} - \text{linear Form} \tag{2}$$

Langmuir isotherm

The results for the Langmuir model are shown in the table. Experiments were performed with 15–90 ppm solutions of sorbate and 1 g of sorbents and the Langmuir model was applied to the results. For chromium removal Langmuir plots and their values are also shown in Figure 7. Negative constant values give the fact that adsorption conditions for these sorbents are different from those assumed for Langmuir isotherm [28].

$$\text{Ce/Cad} = 1/bQ_o + C_e/Q_o \qquad \text{Linear Form} \tag{3}$$

$$\text{Cad} = Q_o bCe/1 + bCe \qquad \text{Non-Linear Form} \tag{4}$$

Elovich isotherm

Linear Elovich calculations were performed on experimental adsorption results for the remediation of Cr (III) by RH, RHBC and HLRHBC. Values of regression constant R^2 and constant Q_m and K_e calculated by using slope and intercept are shown in Table 1. Elovich isotherm was earlier applied for the removal of gases by solid surface adsorbents, but now it is also used to study liquids and solids. A multilayer adsorption process is the main concern of this isotherm. Elovich isotherm plots are also given with R^2 in the order 0.9311 (RHBC) > 0.927 (RH) > 0.9212 (HLRHBC), indicating a

Table 1. Adsorption isotherm parameters for the removal of chromium onto RH, RHBC and HLRHBC.

Adsorbents	Linear isotherm parameters			Non-linear isotherm parameters	
Sorbate	Chromium (III)				
Freundlich	K_f	n	R^2	K_f	n
Raw RH	69.8714	0.166259	0.9513	30.2	2.4
RHBC	336.74	0.383362	0.955	29.4	1.3
HLRHBC	12218	0.163255	0.9696	39.5	1.3
Langmuir	Q_0	b	R^2	Q_0	B
Raw RH	−6.711	−0.9135	0.8641	50.3	0.054
RHBC	−22.026	−1.3926	0.8741	49.5	0.085
HLRHBC	−6.8823	−2.1119	0.8285	43.8	0.232
Elovich	K_e	Q_m	R^2	K_e	Q_m
Raw RH	0.3385	50.76	0.927	0.0422	44.3
RHBC	0.6598	68.02	0.9311	0.078	56.4
HLRHBC	0.7849	51.81	0.9212	0.089	112.3
Dubinin–Radushkevich	K_{ads}	q_s	R^2	K_{ads}	q_s
Raw RH	−1.205	2759	0.9578	−0.469	34.5
RHBC	−0.233	340	0.9371	−0.65	65.49
HLRHBC	−0.534	9417	0.9804	−0.56	76.8
Temkin	K_t	B	R^2	K_t	B
Raw RH	1.335	243.22	0.9138	0.88	16.23
RHBC	3.57	104.64	0.8766	0.18	23.56
HLRHBC	3.06	257.15	0.9747	0.67	28.5

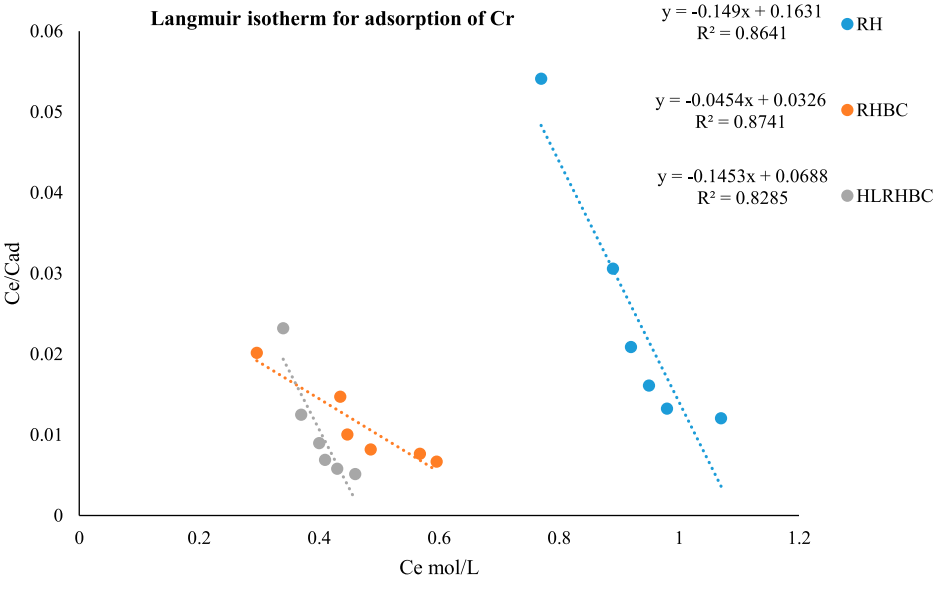

Figure 7. The Langmuir isotherm for the uptake of Cr (III) by RH, RHBC and HLRHBC.

favourable fit. This reveals RH and its other forms served as good adsorbents for chromium removal. Linear and non-linear isotherm values of Elovich constants are given in Table 1 High values of these constants support the model and low values indicate poor

fit (Figure 8).

$$\ln \text{Cad}/\text{Ce} = \ln K_E Q_m - \text{Cad}/Q_m \qquad \text{Linear Form} \qquad (5)$$

$$\text{Cad}/q_m = K_E C_e \exp(-q_e/q_m) \qquad \text{Non-Linear Form} \qquad (6)$$

Dubinin–Radushkevich isotherm model

This model was used to study the best fit for Cr (III) adsorption by the use of various adsorbent materials (Figure 9). R^2 value and constants value q_s and K_{ads} were obtained from slope and intercept by plotting LN Cad and R^2. Plot among adsorption capacity and adsorption concentration gives Dubinin isotherm. The values of the correlation coefficient are in the range of $0.9804 > 0.9578 > 0.9371$, indicating the best fit of data with the Dubinin–Radushkevich isotherm.

$$\ln(\text{Cad}) = \ln(q_s) - k_{\text{ad}} \qquad \text{Linear Form} \qquad (7)$$

$$\text{Cad} = (q_s)\exp(-k_{\text{ad}}\epsilon) \qquad \text{Non-Linear Form} \qquad (8)$$

Temkin isotherm

The results of adsorption experiments were used to find the fit of chromium adsorption into the linear and non-linear forms of the Temkin isotherm. $R^2 = 0.9138$ for RH and 0.9747 for HLRHBC shows favourable adsorption and the best fit for the Temkin isotherm. The heat of adsorption constant $B = 257.15$ for adsorption of chromium onto HLRHBC, assumes the best fit of the model for adsorption, as shown in Figure 10. Heat energy adsorption constant K_t values are also given in the table which reveals favourable data for isotherm. For nonlinear

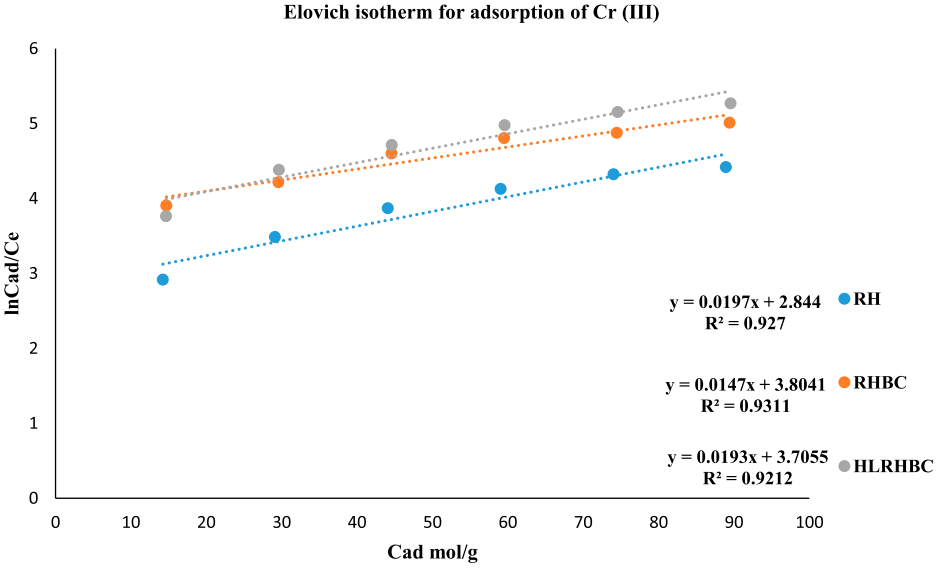

Figure 8. The Elovich isotherm model for the uptake of Cr (III) by RH, RHBC and HLRHBC.

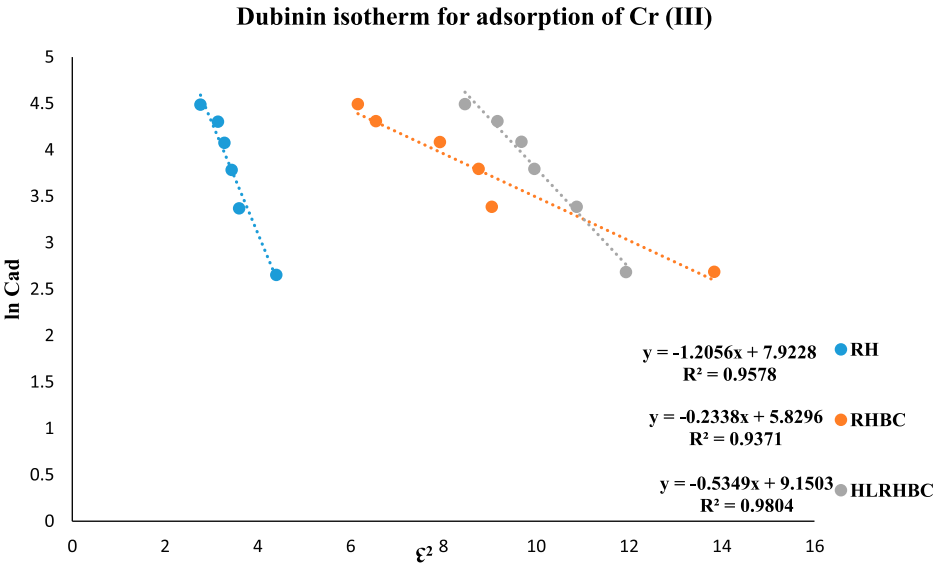

Figure 9. The Dubinin–Radushkevich isotherm for the removal of chromium (III) by RH, RHBC and HLRHBC.

data k_t, constant values are in the range of 0.18–0.88 and B values are in the range of 16.23–28.5 which follows the requirements of the Temkin isotherm.

$$\text{Cad} = \text{RT}/\Delta Q \ln K_T + (\text{RT}/\Delta Q) \ln C_e \quad \text{Linear Form} \tag{9}$$

$$\text{Cad} = \text{RT}/\Delta Q \ln K_T C_e \quad \text{Non-Linear Form} \tag{10}$$

The R^2 value of different isotherms for the removal of **chromium** by various forms of adsorbents is shown below:

RH, R^2 = Freundlich > Dubinin–Radushkevich > Elovich > Temkin > Langmuir
RHBC, R^2 = Freundlich > Dubinin–Radushkevich > Elovich > Temkin > Langmuir
HLRHBC, R^2 = Dubinin–Radushkevich > Freundlich > Temkin > Elovich > Langmuir

Kinetic models

Kinetic models are important to study metal uptake on adsorption sites of adsorbent during a specific time period, and also the effects of particle diffusion and transfer of ions/molecules are studied (Figure 11).

i Pseudo-first -order model (PFO)

Mathematical expression for the pseudo-first-order model is given as follows:

$$(\log q_e - q_t) = \log (q_e) - k_1/2.303{*}t \tag{11}$$

where q_e (mg/g) is the quantity of solute sorbed on the adsorbent surface at an equilibrium state, q_t (mg/g) is the quantity of solute sorbed at time interval t and k_1 is the

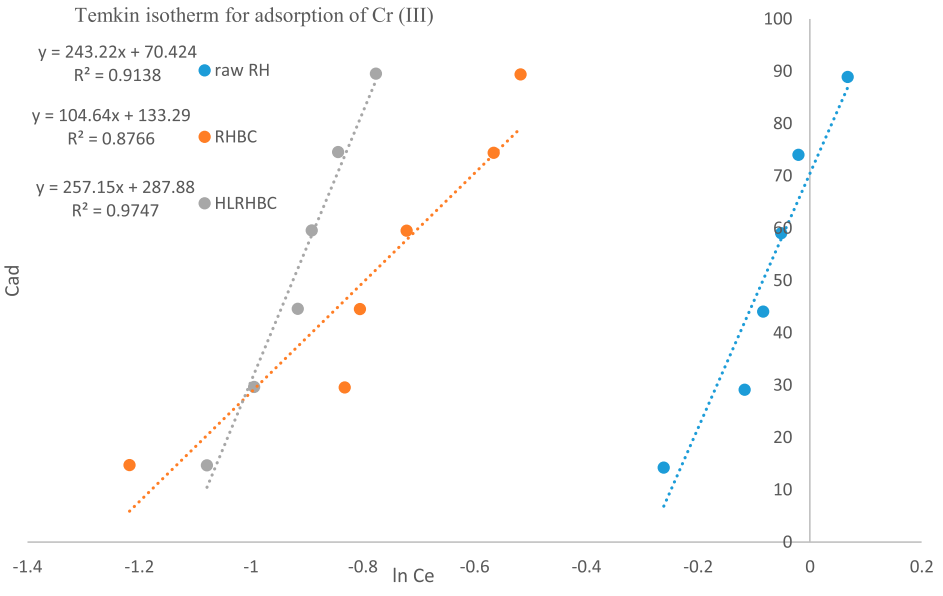

Figure 10. The Temkin model for the uptake of chromium (III) by RH, RHBC and HLRHBC.

adsorption rate constant at time *t*. slope and intercept of the graph plotted for experimental data give values of q_e and k_1.

ii. Pseudo-second -order model (PSO)

The mathematical expression for the pseudo-second-order model is given as follows:

$$t/q_t = 1/\ k_2 qe^2 + (1/q_e)t \tag{12}$$

The initial rate of adsorption is represented by the following equation:

$$h = k_2 qe^2 \tag{13}$$

k_2 = adsorption rate constant, qe adsorption capacity at equilibrium [29].

i Raw RH

The straight line plot was obtained for PFO and PSO models for the adsorption of chromium onto RH. The plots indicated a better fit of the PSO model than PFO because the R^2 value of PSO is close to unity. The estimated results of kinetic parameters obtained from the slope and intercept of the graph are given in Table 2. k_2 values are in the order $0.0050 < 0.0062 < 0.0075 < 0.0080$ for PSOI < III < IV < II and Q_e values are $19.88 > 19.18 > 18.57 > 18.34$ for PSO I > III > IV > II, suggesting the best fit of PSOI into experimental results. PFO also favours results due to the correlation coefficient and lower k_1 value.

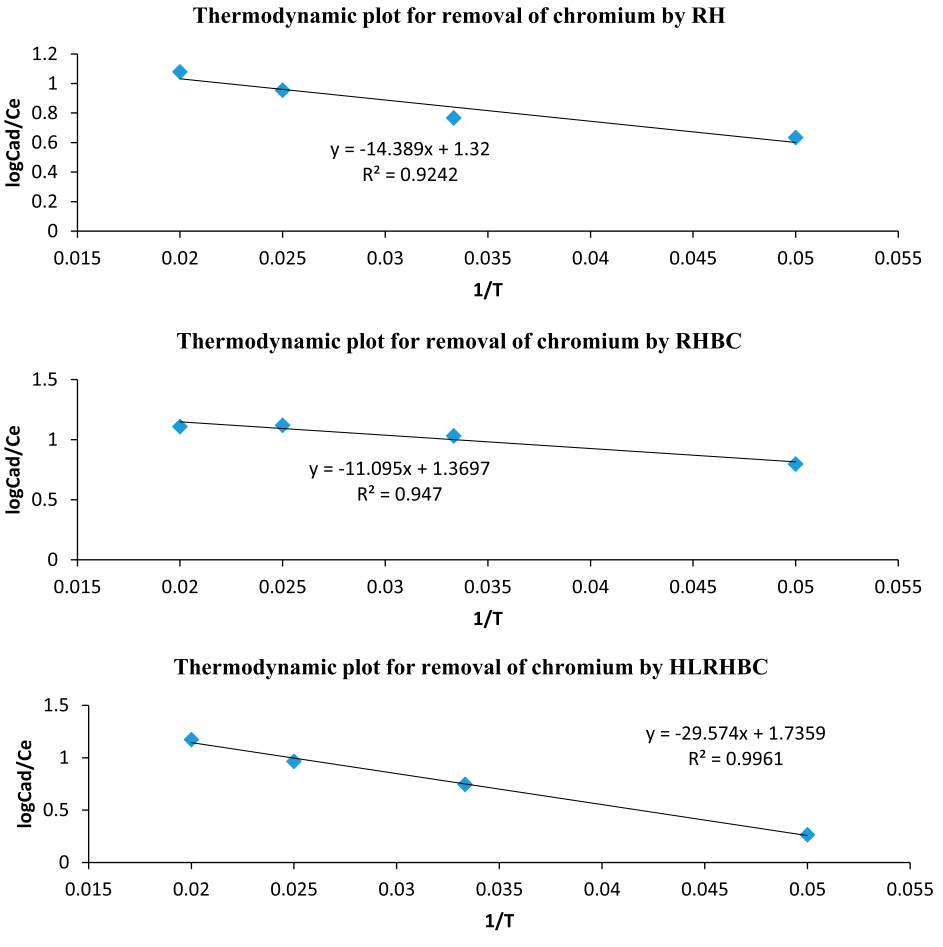

Figure 11. Thermodynamic study for the adsorption of Cr (III) onto a. RH; b. RHBC; c. HLRHB.

ii. RHBC

A time change parameter was also applied to remove chromium from aqueous media by using RHBC sorbent. Experimental data were applied to reveal a better fit kinetic model. R^2 values were in the range of $0.9923 > 0.977 > 0.9651 > 0.9157 = 0.9157$ for PSOI > PFO > PSOII > PSO III = IV, respectively. Kinetic parameters were obtained from the slope and intercept of graphs and their data are in the order Q_e $20.96 > 20.02 > 10.59 > 19.31$ for PSOI > III > IV > II, K_2 $0.0038 < 0.0049 < 0.0054 < 0.0058$ for PSOI < III < IV < II and h values are in the order $1.68 < 1.97 < 2.11 < 2.19$ for PSO I < III < IV < II. These data reveal PSO best fit for the PFO model (Table 3)

iii. HLRHBC

Straight line plots for the adsorption of chromium onto HLRHBC were obtained for PFO and PSO kinetics and parameters k_1, k_2, Q_e and h values are given in Table 4. These values suggest the PSO model has $R^2 = 0.9925$ close to unity and provide the best fit for adsorption data.

Table 2. Kinetic factors for Cr (III) adsorption by RH.

	Kinetic constants			
Pseudo-second-order model (PSO)	R^2	k constant	Q_e	h constant
Type I	0.9952	0.0050	19.88	1.98
Type II	0.9044	0.0080	18.34	2.71
Type III	0.8528	0.0062	19.18	2.31
Type IV	0.8528	0.0075	18.57	2.62
Pseudo-first-order kinetics (PFO)	R^2	k		
	0.9886	−0.0121		

Table 3. Kinetic factors Cr (III) adsorption by RHBC.

	Kinetic constants			
Pseudo-second-order model (PSO)	R^2	k constant	Q_e	h constant
Type I	0.9923	0.0038	20.96	1.68
Type II	0.9651	0.0058	19.31	2.19
Type III	0.9157	0.0049	20.02	2.11
Type IV	0.9157	0.0054	19.59	2.11
Pseudo-first-order kinetics (PFO)	R^2	k		
	0.977	−0.0135		

The following equations were used for calculation

$$\ln(Q_e - Q_t) = \ln(Q_e) - k_1 t \qquad \text{Pseudo First Order Equation}$$

$$\frac{t}{Q_t} = \frac{1}{k_2 Q_e^2} + \left(\frac{1}{Q_e}\right) t \qquad \text{Pseudo Second Order Equation}$$

Thermodynamic study for the adsorption of chromium

When adsorption parameters were studied for the adsorption of chromium onto RH, RHBC and –HLRHBC, the trend revealed a change with a high enthalpy value of 29.57 for HLRHBC and a low value of 11.09 for RHBC. On the contrary, entropy change was high (1.73) for HLRHBC and low (1.32) for RH. Gibbs free energy is negative and decreases with a rise in temperature, to confirm the spontaneity and feasibility of endothermic physical adsorption (Table 5).

Table 4. Kinetic factors for Cr (III) adsorption by HLRHBC.

	Kinetic constants			
Pseudo-second-order model (PSO)	R^2	k constant	Q_e	h constant
Type I	0.9925	0.0031	22.52	1.57
Type II	0.9266	0.0050	20.36	2.09
Type III	0.8666	0.0038	21.54	1.80
Type IV	0.8666	0.0046	20.75	2.00
Pseudo-first-order kinetics (PFO)	R^2	k		
	0.9785	−0.0193		

Table 5. Thermodynamic parameters for the adsorption of chromium on RH, RHBC and HLRHBC.

Sorbents	ΔH (kj/mol)	ΔS (kj/mol K)	ΔG (kj/mol)	Temperature (K)
Raw RH	14.38	1.32	−401.14	293
			−414.34	303
			8	313
			−447.34	328
RHBC	11.09	1.36	−412.5	293
			−426.2	303
			−439.9	313
			−460.45	328
HLRHBC	29.57	1.73	−536.46	293
			−553.76	303
			−571.06	313
			−597.01	328

Table 6. Desorption (%) of Cr (III) from the filtrate.

Sorbent	First	Second	Third	Fourth	Fifth
RH	91.0	86.0	82.0	76.0	73.0
RHBC	92.0	85.0	83.0	79.0	72.0
HLRHBC	92.5	84.0	81.0	74.0	70.0

Desorption of chromium

For chromium desorption nitric acid and deionised water were used. After the first wash removal percentage was 91%, 92% and 92.5% for RH, RHBC and HLRHBC, respectively. The method was repeated for the second, third, fourth and fifth washes. Desorption results are given in Table 6.

Conclusions

This study indicated that HLRHBC was successfully applied for the remediation of chromium metal from an aqueous solution. Three different forms of rice husk, RH, RHBC and HLRHBC, were used for the adsorption processes. Characterisation of adsorbents revealed a large surface area and porosity for HLRHBC then RH and RHBC. Also the FTIR analysis before and after sorption revealed that carboxyl, aldehyde/ketone and C–H are major functional groups that caused the metal binding to the adsorbent surface. Experimental factors, such as, initial metal concentration, time and kinetics showed the rate of the adsorption process and uptake capacity of metal onto the nanomaterial surface. Adsorption increased with an increase in metal ion concentration and its efficiency was high for HLRHBC. Adsorption data were fitted best in the Freundlich isotherm with $R^2 = 0.9696$ high for HLRHBC. Dubinin–Radushkevich and Temkin's isotherms also supported adsorption as indicated by favourable constants values. Linear and non-linear PFO and PSO models were applied to adsorption data. Both models favoured results but the pseudo-second-order model revealed large values of the correlation coefficient compared to the pseudo-first-order model followed by feasible biosorption. Thermodynamic investigations revealed an enthalpy change of 29.57, entropy change of 1.73 and free energy change of −536.46 to −597.01, favouring the spontaneous physical sorption process. These values are high and progressive for HLRHBC compared to RH and RHBC

sorbents. It indicates its benefit in use as small quantity nanomaterial with a large surface area to support metal uptake. A desorption study was performed successfully to recover adsorbent and metal, with a maximum recovery percentage.

Acknowledgements

I sincerely thank Dr. Shahid Iqbal Professor of Chemistry, University of Education Jauharabad, for providing me with superb guidance for conducting research and writing the article. I also thank Dr. Fozia Batool, Assistant Professor, the University of Sargodha for facilitating me at each step of research work and writing. I also thank the University of Sargodha, Sargodha for providing all apparatus and instrument.

Disclosure statement

No potential conflict of interest was reported by the author(s).

Notes on contributors

Dr Tunzeel Iqbal Lecturer in chemistry at department of chemistry The Rawalpindi Women University, Rawalpindi.

Dr Fozia Batool Assistant Professor in chemistry at Institute of chemistry at University of Sargodha, Sargodha.

Dr Shahid Iqbal Professor in chemistry at University of education.

ORCID

Tunzeel Iqbal http://orcid.org/0000-0001-8190-0913
Fozia Batool http://orcid.org/0000-0001-8023-7558
Shahid Iqbal http://orcid.org/0000-0001-5681-5995

References

[1] Sobeih MM, El-Shahat MF, Osman A, et al. Glauconite clay-functionalized chitosan nanocomposites for efficient adsorptive removal of fluoride ions from polluted aqueous solutions. RSC Adv. 2020;2020(10):25567–25585.
[2] Nassar MY, El-Salhy HI, El-Shiwiny WH, et al. Composite nanoarchitectonics of magnetic silicon dioxide-modified chitosan for doxorubicin delivery and in vitro cytotoxicity assay. J Inorg Organomet Polym Mater. 2022: 1–17.
[3] Luther W. Application of nano-technologies in the energy sector; Hessen-Nanotech of the Hessian Ministry of Economy, Transport, Urban and Regional Development. 2008; 88: Wiesbaden, Germany.
[4] Sjostrom E. Wood chemistry: fundamentals and applications. Gulf professional Publishing; 1993.
[5] Lua AC, Yang T, Guo J. Effects of pyrolysis conditions on the properties of activated carbons prepared from pistachio-nut shells. J Anal Appl Pyrolysis. 2004;72:279.
[6] Huq EA. Compilation of environmental laws of Bangladesh. Department of Environment, Government of Bangladesh; 2004.
[7] Muchuweti M, Birkett JW, Chinyanga E, et al. Heavy metal content of vegetables irrigated with mixtures of wastewater and sewage sludge in Zimbabwe: implications for human health. Agric Ecosyst Environ. 2006;112:41.

[8] Aziz HA, Adlan MN, Ariffin KS. Heavy metals (Cd, Pb, Zn, Ni, Cu and Cr (III)) removal from water in Malaysia: post treatment by high quality limestone. Bioresour Technol. 2008;99:1578.
[9] Ahmed MB, Zhou JL, Ngo HH, et al. Competitive sorption affinity of sulfonamides and chloramphenicol antibiotics toward functionalized biochar for water and wastewater treatment. Bioresour Technol. 2017;238:306.
[10] Mohan D, Kumar H, Sarswat A, et al. Cadmium and lead remediation using magnetic oak wood and oak bark fast pyrolysis bio-chars. Chem Eng. 2014;236:513.
[11] Babel S, Kurniawan TA. Low-cost adsorbents for heavy metals uptake from contaminated water: a review. J Hazard Mater. 2003;97:219.
[12] Gomez-Serrano V, Macias-Garcia A, Espinosa-Mansilla A, et al. Adsorption of mercury, cadmium and lead from aqueous solution on heat-treated and sulphurized activated carbon. Water Resour. 1998;32:1.
[13] Tang DS, Zhang L, Chen HL, et al. Extraction and purification of solanesol from tobacco:(I). extraction and silica gel column chromatography separation of solanesol. Sep Purif Technol. 2007;56:291.
[14] Crini G. Recent developments in polysaccharide-based materials used as adsorbents in wastewater treatment. Prog Polym Sci. 2005;30:38.
[15] Volesky B. Biosorption and me. Water Resour. 2007;41:4017.
[16] Sankar S, Sharma SK, Kaur N, et al. Biogenerated silica nanoparticles synthesized from sticky, red, and brown rice husk ashes by a chemical method. Ceram Int. 2016;42:4875.
[17] Yalcin N, Sevinc V. Studies on silica obtained from rice husk. Ceram Intl. 2001;27:219.
[18] Nassar MY, Ahmed IS, Raya MA. A facile and tunable approach for synthesis of pure silica nanostructures from rice husk for the removal of ciprofloxacin drug from polluted aqueous solutions. J Mol Liq. 2019;282:251–263.
[19] Iqbal T, Iqbal S, Batool F, et al. Utilization of a newly developed nanomaterial based on loading of biochar with hematite for the removal of cadmium ions from aqueous media. Sustanability. 2021;13:2191.
[20] Mohammadi-Kalalagh SS, Babazadeh H, Nazemi A. Comparison of linear and nonlinear forms of isotherm models for Zn (II) and Cu (II) sorption on a kaolinite. arab. J Geosci. 2015;8:397.
[21] Popoola LT. Characterization and adsorptive behaviour of snail shell-rice husk (SS-RH) calcined particles (CPs) towards cationic dye. Heliyon. 2019;5:e01153.
[22] Ho YS. Selection of optimum sorption isotherm. Carbon N Y. 2004;42:2115.
[23] Nassar MY, Khatab M. Cobalt ferrite nanoparticles via a template-free hydrothermal route as an efficient nano-adsorbent for potential textile dye removal. RSC Adv. 2016;6:79688–79705.
[24] Refat NM, Nassar MY, Sadeek SA. A controllable one-pot hydrothermal synthesis of spherical cobalt ferrite nanoparticles: synthesis, characterization, and optical properties. RSC Adv. 2022;12:25081–25095.
[25] Ahmad M, Rajapaksha AU, Lim JE, et al. Biochar as a sorbent for contaminant management in soil and water: a review. Chemosphere. 2014;99:19–33.
[26] Wang C, Wang H. Carboxyl functionalized *Cinnamomum camphora* for removal of heavy metals from synthetic wastewater-contribution to sustainability in agroforestry. J Clean Prod. 2018;184:921–928.
[27] Igwe JC, Abia AA. Adsorption isotherm studies of Cd (II), Pb (II) and Zn (II) Ions Bioremediation from Aqueous Solution Using Unmodified and EDTA-Modified Maize cob. Eclét Quím J. 2007;32:33–42.
[28] Oros I, Krstić J, Kovačević I. Adsorption feasibility in the Cr (total) ions removal from waste printing developer. Glob Nest J. 2012;14:18–23.
[29] Kowanga KD, Gatebe E, Mauti GO, et al. Kinetic, sorption isotherms, pseudo-first-order model and pseudo-second-order model studies of Cu (II) and Pb (II) using defatted moringa oleifera seed powder. J Phytopharm. 2016;5:71–78.